Contents lists available at ScienceDirect

Journal of Quantitative Spectroscopy and Radiative Transfer

journal homepage: www.elsevier.com/locate/jqsrt

First HFC-134a retrievals from ground-based FTIR solar absorption spectra, comparison with TOMCAT model simulations, *in-situ* AGAGE observations, and ACE-FTS satellite data for the Jungfraujoch station

Irene Pardo Cantos [a,*], Emmanuel Mahieu [a], Martyn P. Chipperfield [b,c], Christian Servais [d], Stefan Reimann [e], Martin K. Vollmer [e]

[a] Department of Astrophysics, Geophysics, and Oceanography, UR SPHERES, University of Liège, Liège, Belgium
[b] School of Earth and Environment, University of Leeds, Leeds, UK
[c] National Centre for Earth Observation, University of Leeds, Leeds, UK
[d] Department of Astrophysics, Geophysics, and Oceanography, UR STAR, University of Liège, Liège, Belgium
[e] Laboratory for Air Pollution and Environmental Technology, Empa, Swiss Federal Laboratories for Materials Science and Technology, Switzerland

ARTICLE INFO

Keywords:
HFC-134a
NDACC
TOMCAT/SLIMCAT
FTS
AGAGE, Trends

ABSTRACT

Successive regulations on the production and consumption of chlorofluorocarbons (CFCs) and hydrochlorofluorocarbons (HCFCs) have led to the use of hydrofluorocarbons (HFCs) as substitution products. Consequently, these potent greenhouse gases are now controlled under the Kigali Amendment (2016) to the Montreal Protocol. HFC-134a is the preferred substitute to CFC-12 as a refrigerant and is the most abundant HFC in the atmosphere today. This work presents the first retrievals from ground-based Fourier Transform InfraRed (FTIR) high-resolution solar absorption spectra, recorded at the Jungfraujoch station as part of the Network for the Detection of Atmospheric Composition Change (NDACC). To verify these retrievals, the FTIR time series was compared to three other datasets: a simulation of the TOMCAT 3-D chemical transport model, the Fourier Transform Spectrometer on board the Atmospheric Chemistry Experiment (ACE-FTS) L2 v5.2 retrievals, and the Jungfraujoch *in-situ* surface observations conducted within the Advanced Global Atmospheric Gases Experiment (AGAGE) network. The overall trends of HFC-134a (2004–2022) were analyzed to assess the relative growth rates of this atmospheric compound. These trends are 7.34 ± 0.16 %/year (FTIR), 7.12 ± 0.05 %/year (TOMCAT), 7.29 ± 0.16 %/year (ACE-FTS), and 6.61 ± 0.05 %/year (*in-situ*). The relative trends are in good agreement, so these novel FTIR retrievals are validated. Consequently, this strategy could be implemented at other NDACC sites to achieve a quasi-global detection of this species using the FTIR remote sensing technique.

1. Introduction

Since the discovery of the implication of chlorofluorocarbons (CFCs) in stratospheric ozone depletion by Molina and Rowland (1974) [1], the Montreal Protocol on Substances that Deplete the Ozone Layer (1987) has aimed to limit the production and consumption of CFCs and other Ozone-Depleting Substances (ODSs) to protect the ozone layer and allow it to recover. The industry has therefore developed and produced substitutes for CFCs, the hydrochlorofluorocarbons (HCFCs). These substances have shorter atmospheric lifetimes and convey less chlorine atoms on a per molecule basis, which is why they are characterized by smaller ozone depletion potentials (ODPs). Still, HCFCs contribute to stratospheric ozone depletion, which led to their ban. Consequently, hydrofluorocarbons (HFCs), which are chlorine- and bromine-free molecules that do not affect the ozone layer, have been introduced to replace both CFCs and HCFCs [2]. Nevertheless, all these substances are strong infrared (IR) radiation absorbers and hence contribute to the Earth's radiative forcing [3]. As HFCs are very potent greenhouse gases, they were included in the list of substances controlled by the Kyoto Protocol (1997), but no emission limits were established. Therefore, the Kigali Amendment (2016) to the Montreal Protocol came into force in 2019 to gradually reduce the global production and use of long-lived HFCs [4]. HFCs are mainly used in refrigeration systems, air conditioning, and foam-blowing as well as firefighting agents and propellants

* Corresponding author.
E-mail address: i.pardocantos@uliege.be (I. Pardo Cantos).

https://doi.org/10.1016/j.jqsrt.2024.108938
Received 14 November 2023; Received in revised form 7 February 2024; Accepted 9 February 2024

[4]. In the last years, the consumption and emissions of CFCs have decreased. While HCFC consumption and emissions have stabilized in recent years, those of the HFCs continue to rise [4]. Since 2000, global HFC emissions estimated from atmospheric observations show a significant gap to the total CO_2-eq HFC emissions reported by Annex I countries to the United Nations Framework Convention on Climate Change (UNFCCC) in 2019 (Figure 2-2 in [5]). Unfortunately, this gap between estimated and reported emissions has been broadening in the recent years. This difference could be explained by emissions from non-Annex I countries and/or by unrecorded emissions, considering that many countries still do not report to the UNFCCC or remain not monitored by atmospheric observations [4]. The total CO_2-equivalent emissions (based on 100-yr time horizon Global Warming Potential, GWP) by HFCs in 2020 has been estimated to be 1.22 ± 0.05 Gt CO_2-eq yr^{-1} [4].

1,1,1,2-Tetrafluoroethane or CH_2FCF_3 (HFC-134a) has replaced CFC-12 as the preferred refrigerant and is the most abundant HFC in the atmosphere [4]. Its total atmospheric lifetime is 13.5 years (14.1 years in the troposphere and 313 years in the stratosphere) [6]. The large difference between the tropospheric and the stratospheric lifetimes is due to the reaction with tropospheric OH, the main atmospheric sink for HFC-134a (responsible for 99 % of its atmospheric degradation) [2]. Atmospheric HFC-134a loss produces COF_2, HF and trifluoroacetic acid (TFA; CF_3COOH). This is a toxic breakdown product that accumulates in water reservoirs through wet deposition. However, it is known that the environmental impact of TFA still needs to be investigated [7]. It is estimated that HFC-134a emissions started in the early 1990s as the atmospheric HFC-134a levels began to rise in the mid-1990s. This is based on global *in-situ* measurements by NOAA (National Oceanic and Atmospheric Administration) [8,9]. The GWP of HFC-134a is 1470 (100-yr) and it is the largest contributor to radiative forcing from HFCs with 44 % of their total contribution (44.1 ± 0.6 mW m^{-2}) in 2020, which is about 30 % more than in 2016. The share of HFC-134a in total HFCs emissions in 2020 is about 30 %, which is an increase of about 20 % since 2016 [4]. Global emissions of HFC-134a estimated by the Advanced Global Atmospheric Gases Experiment (AGAGE) and NOAA networks are, 247 ± 28 Gg yr^{-1} (or 364 ± 41 Tg CO_2-eq yr^{-1}) and 243 ± 27 Gg yr^{-1} (or 358 ± 39 Tg CO_2-eq yr^{-1}), respectively in 2020 [4].

In this work, we describe the first retrieval strategy from ground-based Fourier Transform InfraRed (FTIR) solar absorption spectra, and we analyze the HFC-134a atmospheric abundances above the Jungfraujoch station. To evaluate this first HFC-134a FTIR time series, we compare our retrieved total columns (presented as dry air mole fractions) to surface air measurements (AGAGE), satellite data (ACE-FTS instrument on board SCISAT) over Europe and TOMCAT model simulations for the period from January 2004 to December 2022. In Section 2, we describe the FTIR, *in-situ* and satellite observations as well as the 3-D chemical transport model. In Section 3, we describe the retrieval strategy, and in Section 4, we present the results and discuss the trend analysis for the different datasets. Finally, we conclude this study in the section "Summary and conclusions".

2. Measurement methods and datasets

2.1. NDACC FTIR observations at the Jungfraujoch station

The FTIR spectra used in this study were recorded under clear-sky conditions at the Jungfraujoch research station (46.55°N, 7.98°E) in the Swiss Alps at 3580 m above mean sea level (a.m.s.l.). The Jungfraujoch station is located between the Mönch (4107 m) and the Jungfrau (4158 m) summits, in a very dry area compared to other NDACC stations, due to the high altitude and the proximity of the Aletsch glacier [10]. Spectra have been recorded since the early 1950s by the team of the Institute of Astrophysics of the University of Liège (Belgium). The high-resolution FTIR measurements began in 1984 [11] and are now conducted as part of the Network for the Detection of Atmospheric Composition Change (NDACC) [12]. The retrievals presented in this article were obtained from a subset of high-resolution infrared solar absorption spectra recorded with a Bruker IFS-120HR spectrometer, modified by the team, and in operation since the early 1990s. These observations were made with a HgCdTe (mercury cadmium telluride, MCT) detector and they cover the 700–1400 cm^{-1} spectral range with a spectral resolution of 0.0061 cm^{-1}, that is a maximum optical path difference (OPD) of 82 cm.

2.2. AGAGE in-situ observations at the Jungfraujoch station

In addition to measurements by FTIR, fully independent observations of HFC-134a at Jungfraujoch are also available through *in-situ* measurements using preconcentration gaschromatography–mass spectrometry (GCMS) [13]. As part of a suite of ~50 halogenated substances, high-precision HFC-134a measurements have been conducted within the AGAGE network [14]. At Jungfraujoch, measurements began in 2000 using a GCMS-ADS (adsorption/desorption) system [15] followed by Medusa-GCMS technology in 2008 [14,16]. For the Medusa-GCMS, 2 L samples are preconcentrated on a first trap and held at ~ –160 °C. The samples are desorbed at 100 °C and cryofocussed on a second trap before injection into the GCMS. The measurement of one sample takes about 70 min. After each pair of air samples, a calibration gas (quaternary standard) is measured to track and correct for MS signal drift. Measurement precision for HFC-134a is about 0.3 % (1-σ). The HFC-134a measurements are fully intercalibrated within the AGAGE network and are reported as dry-air mole fraction in pmol mol^{-1} (parts-per-trillion, ppt) on the Scripps Institution of Oceanography (SIO) calibration scale SIO-05 with an estimate accuracy of ~2 %. For the present study, only baseline measurements (deemed representative for a broad atmospheric region) were used, based on a statistical filtering algorithm [17,18].

2.3. ACE-FTS observations

The ACE-FTS instrument on board the Atmospheric Chemistry Experiment (ACE), also known as SCISAT, is the main instrument of this Canadian satellite [19]. SCISAT was launched into low Earth circular orbit by NASA in August 2003. Since February 2004, this satellite has been collecting data of the atmospheric pressure, temperature, and several molecular abundances [20]. ACE-FTS is a Fourier Transform Spectrometer (FTS) that records up to 30 IR transmittance spectra per day at sunrise and sunset by solar occultation. The locations of the occultations are determined by the orbit of the satellite and its relative position to the Sun [2]. This instrument operates in the range from 750 to 4400 cm^{-1} with a spectral resolution of 0.02 cm^{-1} [20]. The signal-to-noise ratio (SNR) ranges from about 100:1 to about 400:1 [21]. The vertical resolution averages about 3 km and each occultation analyzes the atmosphere from 150 km down to the cloud tops, or down to 5 km at best under clear-sky conditions [2]. Five micro-windows (MW) are used for the HFC-134a retrievals: MW_1 = 828.78–829.28 cm^{-1}; MW_2 = 1090.20–1090.60 cm^{-1}; MW_3 = 1103.04–1105.84 cm^{-1}; MW_4 = 1949.93–1950.28 cm^{-1}; and MW_5 = 2623.63–2624.28 cm^{-1} [20]. For this study, we used ACE-FTS Level 2 v5.2 retrievals of the HFC-134a molecular abundances, expressed as volume mixing ratios (VMRs), from 5.5 km to 15.5 km for a latitude band around the Jungfraujoch station (40–50°N). We limited the ACE-FTS measurements to 15.5 km because the vertical profile decreases meaningfully above this altitude [19,2]. Further information on the ACE-FTS version 5 retrievals can be found in Boone et al. (2023) [21].

2.4. The TOMCAT/SLIMCAT chemical transport model

To help interpret the observations, we used output from a simulation of the TOMCAT/SLIMCAT (hereafter TOMCAT) three-dimensional (3-D) chemical transport model (CTM) [22]. The simulation used here had a horizontal resolution of 2.8° × 2.8° with 32 levels from the surface to ~ 60 km. The model was forced using meteorology from European Centre

for Medium-Range Weather Forecasts (ECMWF) ERA5 reanalyses [23] and was integrated from 1979 until 2022. The model contained a detailed treatment of stratospheric chemistry including interactive calculation of photochemistry (OH, photolysis) relevant for HFCs.

The model run was constrained by specifying the monthly mean global mean surface VMRs of the long-lived source gases. For species such as CFCs and HCFCs these are taken from the Scientific Assessment of Ozone Depletion (2018) [24]. For HFCs, including HFC-134a, the global mean surface VMRs are taken from the NOAA Annual Greenhouse Gas Index (data obtained from https://gml.noaa.gov/aggi/aggi.html). This boundary condition constraint means that the model does not simulate the spatial and short-term temporal variation in the surface concentration of HFC-134a. The model does, however, simulate the relative HFC-134a profile shape through atmospheric transport and loss processes. For comparison with observations the simulated model profile was sampled daily (at 0 UT) at the location of Jungfraujoch.

3. HFC-134a total column retrievals

3.1. Retrieval strategy

Since the main absorber in the infrared domain is water vapor, the dry conditions of the Jungfraujoch station facilitate the detection, retrieval, and analysis of trace gases with very weak spectral absorptions, such as HFC-134a. The application to other NDACC sites has yet to be tested.

We investigated all the significant HFC-134a features included in the pseudo-line list produced by G. C. Toon from the Jet Propulsion Laboratory (https://mark4sun.jpl.nasa.gov/), which is based on six laboratory absorption cross-section datasets from Clerbaux et al. (1993) [25]; Highwood and Shine (2000) [26]; Nemtchinov and Varanasi (2004) [27]; Sharpe et al. (2004) [28]; Gohar et al. (2004) [29]; and Harrison (2015) [30] (https://mark4sun.jpl.nasa.gov/data/spec/Pseudo/HFC-134a_PLL.compressed.pdf). However, only two were suited for the inversion of our ground-based solar atmospheric spectra: 1104.300–1105.585 cm^{-1} and 1182.0–1186.4 cm^{-1}. In this work, we will only present the results for the first window since the second one shows a strong water vapor absorption between about 1185.0 cm^{-1} and 1186.4 cm^{-1}, which masks the main absorption of HFC-134a, even at Jungfraujoch. In addition, the HFC-134a absorption in the second window is smaller and more unstructured than in the first window. Please, consult Figure 1 in the supplementary materials for more information about the second spectral window. The first window range was also used by the ACE-FTS team for the HFC-134a retrievals [20]. To maximize the absorption depth of our target molecule and the information content, only the subset of observations with an apparent solar zenith angle (SZA) between 60° and 85° was fitted. For this work, we did not filter the observations according to water vapor or ozone columns since there is no dependency to the air mass, or the H_2O or O_3 total columns (Figure 2 in the supplementary materials). However, some filtering could be necessary in more humid sites or in sites located at lower altitudes than Jungfraujoch.

For the retrieval of the HFC-134a total columns, we adopted a Tikhonov L1 regularization with an α-parameter of 50. The simulations and retrievals of the total columns were performed using the SFIT-4 v1.0.18 algorithm, which applies the Optimal Estimation Method (OEM) of Rodgers (2000) [31]. The layer scheme spanned 41 layers from 3.58 km to 120 km high, and thickness gradually rose from 0.65 km for the lowest layer up to 14 km for the highest layer.

The simulated interfering species are CO_2, H_2O, O_3, some ozone isotopologues (O3667, O3668, and O3686), formic acid (HCOOH), CH_4, CCl_2F_2 (CFC-12), and $CHClF_2$ (HCFC-22). These interfering molecules were also used for the HFC-134a ACE-FTS retrievals by Fernando et al. (2019) [20]. The spectroscopic parameters for the interfering species were obtained from the HITRAN2020 database [32] and the empirical pseudo-line list created by G. C. Toon for the unresolved features of the halocarbons (https://mark4sun.jpl.nasa.gov/pseudo.html). The spectroscopic parameters of water vapor were obtained from the ATM20 (https://mark4sun.jpl.nasa.gov/specdata.html) compilation.

A priori profiles of the interfering species were obtained from the Whole Atmosphere Community Climate Model (WACCM, version 6; [33]) climatological profiles over the period 1980–2040, except for water vapor. *A priori* profiles of water vapor were supplied by the ERA-Interim [34] and ERA-5 [23] meteorological reanalyzes complemented with WACCMv6 monthly means for the uppermost atmospheric layers. Since HFC-134a is not included in the WACCM simulations, we used the ACE-FTS vertical distribution for 2006 [2] as *a priori* profile for HFC-134a for the upper troposphere and lower stratosphere (5–15 km). The lower tropospheric *a priori* profile was considered constant from the lower limit of ACE-FTS HFC-134a profile (5 km). In the same way, the middle stratospheric *a priori* profile was considered constant from the upper limit of ACE-FTS HFC-134a profile (15 km). Using another year profile, for example 2018 [2], as *a priori* has no measurable effect on the retrieved FTIR products.

Panel B in Fig. 1 shows a simulation of the 1104.300–1105.585 cm^{-1} spectral window. The observed spectrum (obs) is displayed in black and the simulated spectrum (fit) is shown in orange. Each individual molecule is shown in the colors indicated in the legend. As can be observed, the main interferences in this window are due to ozone (in dark green). The absorption feature of HFC-134a (in red, Panel C) peaks around 1104.55 cm^{-1} and 1105.24 cm^{-1}, surrounding the water vapor absorption (in light turquoise) in the center of the window. Even though the interferences from the other molecules appear very weak, we cannot ignore them since the absorption of our target molecule represents only about 1 % (Panel C), so any small contribution from other species can be important for the retrievals. Panel A shows the fitting residuals (observed – calculated) from the simulated spectrum to a spectrum obtained on May 25, 2016. The residuals are close to the noise level, except around some of the most intense ozone absorption lines. The root-mean-square (RMS) of the fitting residuals is 0.27 % and the H_2O total column is 7.3 × 10^{21}molec. cm^{-2} for this example. This spectrum is a good representation of the whole time series (2004–2022), as the median and mean RMS are 0.27 % and 0.28 %, respectively, and the median and the mean H_2O total columns are 5.4 × 10^{21} molec. cm^{-2} and 6.8 × 10^{21} molec. cm^{-2}, respectively. This spectrum was recorded with a maximum OPD of 82 cm at a solar zenith angle of 77.2°, which is at the median of the SZA of the whole spectra used in this study.

3.2. Uncertainty analysis of the measurements

The main sources of error affecting the retrievals of the total columns are listed in Table 1. This uncertainty budget was calculated for one year of spectra (2014), taken as an example in the middle of the time series. The random and systematic components are presented separately. To create the random component of the error covariance matrix, we used a constant relative standard deviation of 18 %, based on ACE-FTS L2 v5.2 HFC-134a retrievals [21], for each level of the grid (1 km-levels between 5.5 and 15.5 km; between 40 and 50°N) which represents the average relative standard deviation for four months of the ACE-FTS time series (April–July 2012). The systematic part was produced using the mean relative difference between the ACE-FTS L2 v5.2 HFC-134a retrievals and the TOMCAT simulations in the lowest model layer for the same four months. The model simulations were used for this estimation as no other satellite observations are currently available. A constant relative difference of 10 % was used for each layer of the grid. This value is similar to the systematic component used for HCFC-22 by Prignon et al. (2019) [35]. The correlation width of the HFC-134a profile was assumed to be 3 km. The random uncertainty for the SZA was set to ±0.1°, while the systematic uncertainty was assumed to be ±0.03°. The relative systematic uncertainties of the spectroscopic parameters of HFC-134a (line intensity, temperature, and pressure) were set to 5 %, according to the empirical pseudo-line list produced by G. C. Toon.

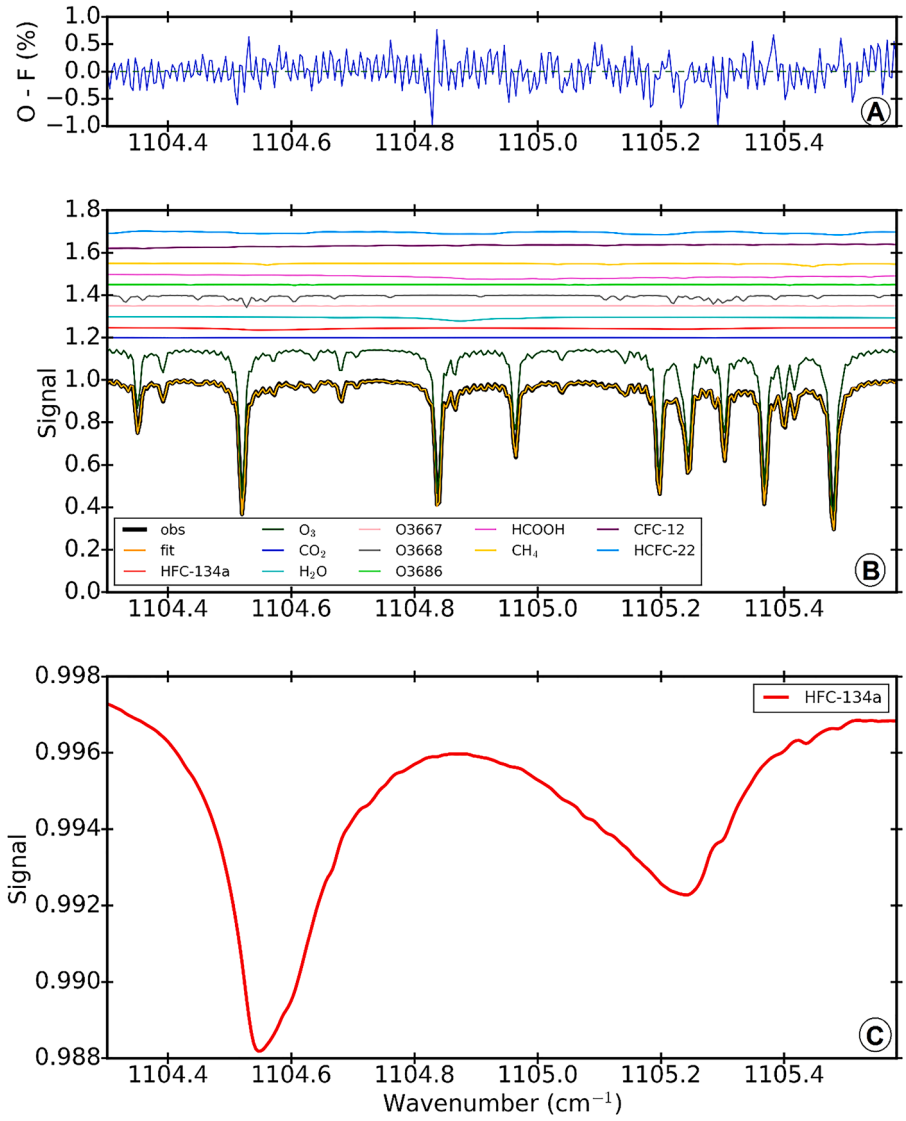

Fig. 1. Spectral window for HFC-134a. Panel A displays the observed – calculated residuals, in %, from the simulation to the spectrum recorded on May 25, 2016. The root-mean-square of the fitting residuals is 0.27 %. Panel B shows the simulation of the 1104.300 – 1105.585 cm^{-1} spectral window for spectra recorded by the Bruker IFS-120HR FTIR instrument at the Jungfraujoch station at an apparent solar zenith angle of 77.2°, and a maximum optical path difference of 82 cm. The signal-to-noise ratio for this spectrum is 952. The main interfering species (O_3, CO_2, H_2O, the ozone isotopologues, HCOOH, CH_4, CFC-12, and HCFC-22) are shifted vertically for clarity. Be aware of the scale of the vertical axis in Panel C, where the HFC-134a absorption is magnified.

Table 1
Mean relative uncertainties (%) for one year (2014) concerning the HFC-134a total column retrievals for the Jungfaujoch station.

	Relative uncertainty (%)	
Error type and source	**Mean**	**Standard deviation**
Random components		
Measurement	6.7	2.2
Temperature	4.3	1.0
SZA	0.8	0.3
Interfering species	5.5	1.9
Smoothing	1.0	0.1
Retrieval parameters	0.3	0.2
Total random	**9.8**	**2.8**
Systematic components		
HFC-134a line intensity	4.99	0.01
Temperature	7.1	1.9
SZA	0.3	0.1
Total systematic	**8.9**	**1.5**

The mean total random and systematic uncertainties are 9.8 ± 2.8 % and 8.9 ± 1.5 %, respectively. The error budgets for 5 years before and after 2014 were also calculated. For 2009, the total random and systematic uncertainties are 14.5 ± 3.8 % and 13.3 ± 3.0 %, respectively, while for 2019, they are 8.5 ± 2.5 % and 7.1 ± 1.1 %, respectively. These results highlight the challenge to retrieve HFC-134a from ground-based FTIR solar absorption spectra in the early 2000s, while the atmospheric load only started to develop in the mid-1990s. Consequently, we decided to show here the HFC-134a total columns above Jungfraujoch from 2004 to 2022, spanning the same period as the ACE-FTS dataset. As shown in Table 1, the random error is mainly determined by the uncertainties of the measurement, the temperature, and the interfering species, while the systematic error is mainly influenced by the uncertainty of the spectroscopic parameters. The other sources of uncertainty only contribute less than 1 % to the total error (random and systematic). These relative uncertainties are determined by dividing the measurement uncertainty by the absolute total column value.

The mean layer averaging kernels provide the information content of the retrieval processing required to characterize the relative weighting

between the *a priori* and the true vertical profiles to the retrieved vertical distribution [31]. Fig. 2 shows the mean layer averaging kernels (left panel) and the first eigenvector (right panel) calculated for the spectra recorded above the Jungfraujoch station in 3 years (2007–2009). The thick black line indicates the total column averaging kernel scaled by 0.1 (from 3.58 km, the station altitude, up to 40 km), while the colored lines show the different individual layer averaging kernels, indicated by the vertical color bar. The degrees of freedom for signal (DOFS) inform on how much information can be extracted from the retrievals. The mean DOFS of the entire time series is 1.0, so the retrievals provide one useful piece of information. The 100 % of the information characterizing the troposphere comes from the retrievals and not from the assumed *a priori*, as indicated by the first eigenvalue ($\lambda_1 = 1.0$).

We also analyzed the effects of the misalignment of the Bruker 120HR spectrometer between July 2011 and December 2012, because the retrieved total columns presented a discontinuity in this period, with a local maximum that was not observed in the other datasets. For this purpose, we retrieved an effective apodization. Nevertheless, this perturbation did not show consistent effects on the retrieved total columns. This effect was also observed in the partial columns of other species retrieved at the Jungfraujoch station during the same period, such as HCFC-22 [35].

4. Results and discussion

In this section, we present the HFC-134a time series obtained after the retrieval of the total columns, as well as the trend analyzes and seasonality. Since these are the first HFC-134a retrievals from ground-based FTIR solar absorption spectra, we compare our results with other three independent datasets, described in Section 2.

4.1. Time series of HFC-134a above the Jungfraujoch NDACC site

With the aim of keeping good spectra, we did not consider data with a fit RMS higher than 0.6 (considering that the mean fit RMS is 0.3). We also removed data from July 2011 to December 2012 due to the low reliability of the retrievals, as explained in the section above. Before filtering, we had 5019 spectra for the whole time series (January 2004–December 2022), i.e. 1542 daily measurements. After filtering, we retained specifically 1382 daily observations (196 months). To use the same units and to easily compare the four independent time series, we show here the FTIR dry air mole fractions (xHFC-134a) instead of the retrieved total columns. These xHFC-134a were determined by dividing the HFC-134a total columns by the dry air pressure column (DPC), which can be obtained as described in Barthlott et al. (2015) [36], and Pardo Cantos et al. (2022) [37]. The water vapor columns used to calculate the xHFC-134a were obtained using a dedicated retrieval strategy for water vapor, described by Sussmann et al. (2009) [38].

4.2. Comparisons with independent datasets

Fig. 3 shows the annual means of the four different datasets from January 2004 to December 2022. As orange dots, the xHFC-134a from FTIR measurements at the Jungfraujoch station; in blue up-pointing triangles, the HFC-134a surface volume mixing ratios derived from TOMCAT model simulations; in purple squares, the HFC-134a VMRs from ACE-FTS for a latitude band between 40 and 50°N (centered around the Jungfraujoch station location) and averaged over an altitude range between 5.5 and 15.5 km; finally, the green down-pointing triangles show the *in-situ* HFC-134a mole fractions measured at the Jungfraujoch station within the AGAGE network. The error bars show the standard deviation around the annual means. The mean relative standard deviations are 9.5 % for the FTIR annual xHFC-134a averages, commensurate with the random uncertainty shown in Table 1; 2.3 % for the annual means of the TOMCAT model surface VMRs; 10.9 % for the ACE-FTS HFC-134a VMRs; and 3.4 % for the *in-situ* baseline mole fractions.

For the FTIR time series, some periods must be emphasized. First, the 2021 annual mean is higher because the spectrometer was out of operation from January to May 2021, so this annual mean only includes the second half of the year, when the atmospheric HFC-134a content is higher, as shown in Fig. 4. In addition, the quality of the spectra from 2021 is less accurate as the maintenance of the Bruker 120HR spectrometer could not be performed frequently enough due to travel restrictions. The second period to note extends from July 2011 to December 2012. This one-and-a-half-year data was suppressed because of the low quality of the retrievals during this period, as explained in Section 3. Consequently, the 2011 xHFC-134a annual mean is slightly lower because we only considered the first half of the year, when the atmospheric HFC-134a burden is lower.

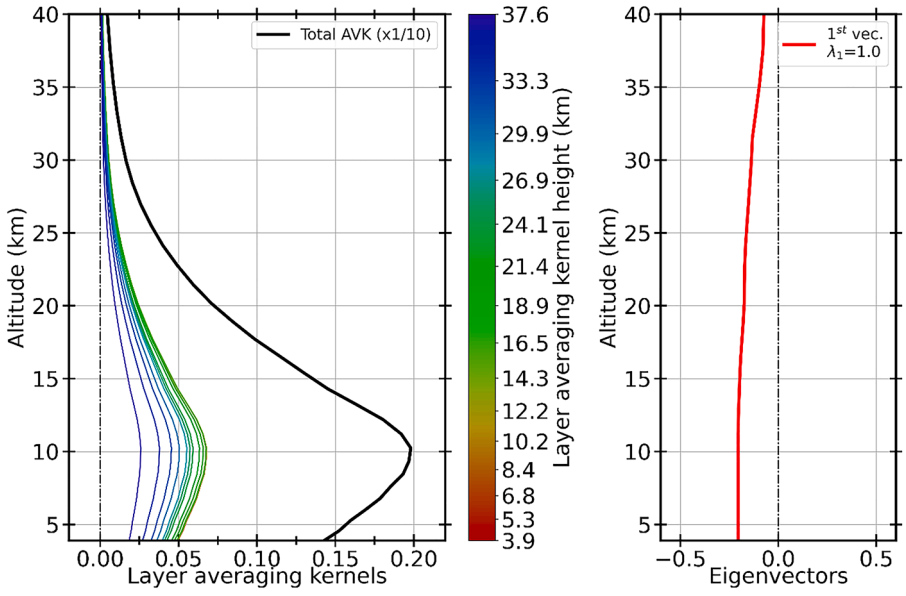

Fig. 2. Mean layer averaging kernels and first eigenvector. The left panel shows the mean layer averaging kernels for mixing ratios computed for the spectra recorded at the Jungfraujoch station from January 2007 to December 2009. The ticks on the color bar are the individual layer averaging kernels represented in the graph. The first eigenvector is shown in the right panel and its eigenvalue is 1.0.

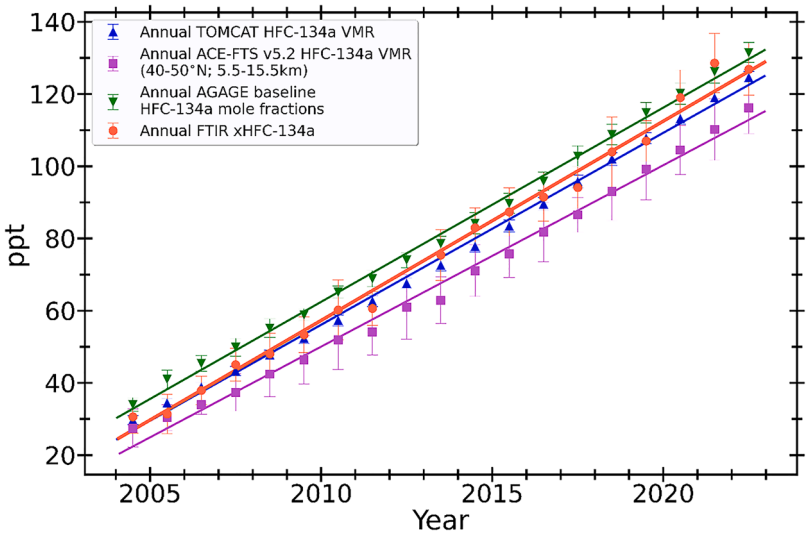

Fig. 3. Atmospheric HFC-134a annual means derived from the different datasets. As orange dots, the Jungfraujoch FTIR xHFC-134a data; as blue up-pointing triangles, the TOMCAT HFC-134a lower-most model level VMRs; as purple squares, the ACE-FTS L2 v5.2 HFC-134a VMRs; and as green down-pointing triangles, the in-situ baseline HFC-134a mole fractions at Jungfraujoch. The vertical error bars depict one standard deviation. The respective linear trends are indicated by the straight lines.

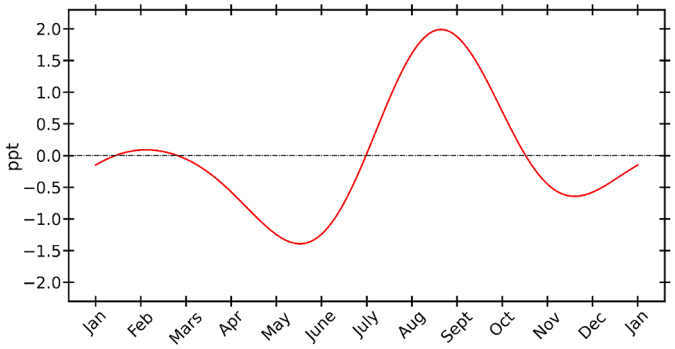

Fig. 4. Seasonal cycle of xHFC-134a as derived from the FTIR observations at the Jungfraujoch station. The minimum atmospheric HFC-134a is at the end of spring, while the maximum occurs at the end of summer.

The FTIR and TOMCAT model time series are in good quantitative agreement. In fact, the mean relative systematic difference between TOMCAT VMRs and FTIR xHFC-134a monthly means is 5.3 %, which is covered by the systematic uncertainty of the retrievals shown in Table 1. This mean relative systematic difference between the two datasets was determined by dividing the difference of the mean TOMCAT and FTIR values by the mean TOMCAT VMR. While the two datasets almost overlap for the earlier years, they diverge slightly later on. Still, the respective trends are consistent when the associated statistical uncertainties are considered. The ACE-FTS time series seems to be down shifted compared to the FTIR series, while the *in-situ* baseline HFC-134a time series is higher than the FTIR time series. However, we should not forget that the ACE-FTS observations mainly represent the upper troposphere, as only a subset of the measured profiles reached down to 5.5 km. While the *in-situ* measurements are representative of the surface mole fractions, the FTIR observations are less sensitive in the first few kilometers of the atmosphere, and they reach a maximum around 10 km to then decrease rapidly above, as shown in Fig. 2. The differences between the four datasets may have several causes including the time required for vertical transport and mixing. The systematic uncertainty reported in Table 1 could also explain part of the bias between the *in-situ* and the remote sensing datasets.

4.3. Trend analyses and seasonality

We analyzed the linear trend of the entire FTIR time series (2004–2022). The trends and their uncertainties were estimated using the autoregressive wild bootstrap method developed by Friedrich et al. (2020) [39] with a 95 % confidence interval. The absolute and relative linear trends are gathered in Table 2. These trends were calculated using the monthly means, even if only the annual means are shown in Fig. 3 for reasons of clarity. The relative trends were calculated by dividing the absolute trend by the mean value (dry air mole fractions, or VMRs, or baseline mole fractions) of the whole time series.

We found that the HFC-134a atmospheric concentration according to the FTIR measurements above the Jungfraujoch site increased by 5.52 ± 0.12 ppt per year, or a relative increase of 7.34 ± 0.16 % per year. Regarding the other time series, a rise of 7.12 ± 0.05 % per year (TOMCAT), 7.29 ± 0.16 % per year (ACE-FTS), and 6.61 ± 0.05 % per year (*in-situ*) was observed. Therefore, the FTIR, TOMCAT and ACE-FTS relative trends agree when we weigh the uncertainties. The *in-situ* relative trend is slightly lower by about 8 %.

Other studies have already analyzed the atmospheric HFC-134a trends (Montzka et al. (2015) [9], Fernando et al. (2019) [20], Harrison et al. (2021) [2]). The Scientific Assessment of Ozone Depletion [4] reports an increase in global HFC-134a from 85.5 ± 0.3 ppt in 2016 to 109.8 ± 0.2 ppt in 2020 in the upper troposphere. A study by Bernath et al. (2021) [40] describes a global trend for the ACE-FTS Level 2 v4.1 HFC-134a retrievals (2004–2020) of 5.71 ± 0.07 ppt per year, that is 6.86 ± 0.22 % per year, which is in line with our results.

Finally, we analyzed the seasonal cycle of xHFC-134a (Fig. 4), which exhibits minimum abundances at the end of spring (May-June), and maximum load at the end of summer (August-September). A local minimum is present in November, and a local maximum in February. It

Table 2
Relative and absolute trends derived for the FTIR xHFC-134a at Jungfraujoch, the TOMCAT surface HFC-134a VMRs, the AGAGE HFC-134a mole fractions at Jungfraujoch, and the ACE-FTS HFC-134a VMRs, for the 2004–2022 period.

Source	Trend (ppt yr^{-1})	Relative trend (% yr^{-1})
xHFC-134a FTIR	5.52 ± 0.12	7.34 ± 0.16
TOMCAT surface VMR	5.32 ± 0.04	7.12 ± 0.05
ACE-FTS v5.2 HFC-134a VMR	5.02 ± 0.11	7.29 ± 0.16
AGAGE baseline mole fractions	5.38 ± 0.04	6.61 ± 0.05

is important to note that the seasonal cycle peak-to-peak amplitude is relatively weak, around 3.5 ppt, that is 4.5 %. This behavior is also captured by the TOMCAT seasonal cycle, where the maximum occurs in early September and the minimum in early April. The annual cycle of the *in-situ* baseline HFC-134a mole fractions at Jungfraujoch shows a minimum at the end of winter and a maximum load during the spring and summer. These *in-situ* baseline measurements can account for the regional emissions and their main sink is oxidation by the OH radical. However, the FTIR measurements are also influenced by the tropopause height and the atmospheric circulation. Above the Jungfraujoch site, the mean tropopause height is around 11.3 ± 2.2 km (2-σ) [41,42]. On the one hand, the tropopause above Jungfraujoch sinks in fall and winter and reaches a minimum height at the beginning of March. On the other hand, the tropopause above the station rises in spring and summer and gets a maximum height in mid-August [41].

5. Summary and conclusions

In this study, we described the retrieval strategy we developed for HFC-134a from ground-based FTIR solar absorption spectra recorded at the high-altitude dry Jungfraujoch station. This was the first attempt to retrieve HFC-134a within the NDACC network. HFC-134a is the most abundant HFC in the atmosphere and the preferred substitute to CFC-12 as a refrigerant. Even though HFCs do not directly affect stratospheric ozone, they are very potent greenhouse gases, which is why they were included in the Kigali Amendment to the Montreal Protocol.

We chose the 1104.300–1105.585 cm^{-1} spectral window for the retrievals, in which the HFC-134a feature typically represents only 1 % of the absorption depth. We chose this window as the water vapor absorption is not very intense, which is an essential point to consider in the cases where the absorption of the target molecule is weak. The main interfering species in this window is ozone and its absorption lines are well defined. The mean DOFS is equal to 1.0, which allows the determination of a single piece of information.

The trend of xHFC-134a was analyzed from January 2004 to December 2022. The previous years were not analyzed because the FTIR retrievals in early 2000 are quite challenging for this molecule, as demonstrated in the error budget analysis section. The obtained FTIR HFC-134a time series was compared to three other independent datasets: TOMCAT model simulations, ACE-FTS satellite observations, and AGAGE *in-situ* surface measurements also performed at the Jungfraujoch station. The calculated trends for the whole time series showed an increase of 7.34 ± 0.16 % per year (FTIR), 7.12 ± 0.05 % per year (TOMCAT), 7.29 ± 0.16 % per year (ACE-FTS) and 6.61 ± 0.05 % per year (*in-situ*). The effects of the Kigali Amendment are not yet visible, as it only came into force in 2019. The seasonal cycle of HFC-134a over the Jungfraujoch showed a maximum atmospheric load at the end of summer and a minimum at the end of spring, which could be driven by the tropopause height.

As reported in the Scientific Assessment of Ozone Depletion (2022) [5], global top-down derived emissions of HFCs show a significant gap with the total HFC emissions reported by Annex I countries to the UNFCCC in 2019. Understanding these differences between the reported and estimated emissions requires continuous atmospheric monitoring in support to the Kigali Amendment. The strategy presented in this manuscript has been validated by comparison with three other independent datasets. It could therefore be implemented at other NDACC sites to achieve quasi-global coverage of this species using the FTIR remote sensing technique.

Research data

The Jungfraujoch FTIR data are available upon request (i.pardo-cantos@uliege.be). The *in-situ* Jungfraujoch data are available at the AGAGE website (https://agage2.eas.gatech.edu/data_archive/agage/). ACE-FTS data are available at the ACE/SCISAT Database (https://databace.scisat.ca/level2/).

CRediT authorship contribution statement

Irene Pardo Cantos: Conceptualization, Data curation, Formal analysis, Investigation, Methodology, Software, Visualization, Writing – original draft. **Emmanuel Mahieu:** Conceptualization, Data curation, Funding acquisition, Investigation, Methodology, Project administration, Supervision, Writing – review & editing. **Martyn P. Chipperfield:** Data curation, Resources, Validation, Writing – review & editing. **Christian Servais:** Software. **Stefan Reimann:** Data curation, Writing – review & editing. **Martin K. Vollmer:** Data curation, Writing – review & editing.

Declaration of competing interest

The authors declare the following financial interests/personal relationships which may be considered as potential competing interests: Irene Pardo Cantos reports financial support was provided by University of Liege. If there are other authors, they declare that they have no known competing financial interests or personal relationships that could have appeared to influence the work reported in this paper.

Data availability

Data will be made available on request.

Acknowledgements

This work was supported by the Fonds de la Recherche Scientifique (F.R.S. – FNRS, Brussels, Belgium) [grant no. J.0126.21], the GAW-CH program of MeteoSwiss (Zürich, CH) and the University of Liège (Belgium). EM is a senior research associate with F.R.S. – FNRS. The ULiège team thanks the International Foundation High Altitude Research Stations Jungfraujoch and Gornergrat (HFSJG, Bern, CH) for supporting the facilities needed to perform the Fourier Transform InfraRed observations at Jungfraujoch. MPC was supported by the UK Natural Environment Research Council SISLAC (NE/R001782/1) and LSO3 (NE/V011863/1) projects. The TOMCAT model runs were performed on the UK Archer and University of Leeds ARC computers. We thank Wuhu Feng (NCAS) for help with the ECMWF meteorology. The AGAGE operation at Jungfraujoch is funded by the Swiss National Programs HALCLIM and CLIMGAS-CH (Swiss Federal Office for the Environment, FOEN), by the International Foundation for High 25 Altitude Research Stations Jungfraujoch and Gornergrat (HFSJG). We thank Dr G. C. Toon for developing, maintaining and making available the pseudo-line lists (PLLs) and the ATM20 spectroscopic compilation that were essential to the present work. The Atmospheric Chemistry Experiment (ACE) is funded by the Canadian Space Agency and we thank the whole team for the ACE-FTS retrievals of HFC-134a.

Supplementary materials

Supplementary material associated with this article can be found, in the online version, at doi:10.1016/j.jqsrt.2024.108938.

References

[1] Molina MJ, Rowland FS. Stratospheric sink for chlorofluoromethanes: chlorine atom-catalysed destruction of ozone. Nature 1974;249:810–2. https://doi.org/10.1038/249810a0.

[2] Harrison JJ, Chipperfield MP, Boone CD, Dhomse SS, Bernath PF. Fifteen years of HFC-134a satellite observations: comparisons with SLIMCAT calculations. J Geophys Res: Atmos 2021;126:e2020JD033208. https://doi.org/10.1029/2020JD033208.

[3] Velders GJ, Daniel JS, Montzka SA, Vimont I, Rigby M, Krummel PB, Muhle J, O'Doherty S, Prinn RG, Weiss RF, Young D. Projections of hydrofluorocarbon

(HFC) emissions and the resulting global warming based on recent trends in observed abundances and current policies. Atmos Chem Phys 2022;22(9):6087–101. https://doi.org/10.5194/acp-22-6087-2022.
[4] Liang Q, Rigby M, et al. Chapter 2: hydrofluorocarbons (HFCs). World Meteorological Organization (WMO). Scientific assessment of ozone depletion: 2022, ozone research and monitoring. Geneva: WMO; 2022. p. 509. GAW Report No. 278.
[5] World Meteorological Organization (WMO). *Scientific assessment of ozone depletion: 2022*, ozone research and monitoring. Geneva: WMO; 2022. p. 509. GAW Report No. 278.
[6] Burkholder JB, Hodnebrog O, et al. Annex: summary of abundances, lifetimes, ODPs, REs, GWPs, and GTPs. World Meteorological Organization (WMO). Scientific assessment of ozone depletion: 2022, Ozone research and monitoring. Geneva: WMO; 2022. p. 509. GAW Report No. 278.
[7] Daniel JS, Reimann S, et al. Chapter 7: scenarios and information for policymakers. World Meteorological Organization (WMO). Scientific assessment of ozone depletion: 2022, Ozone Research and Monitoring, GAW Report No. 278. Geneva: WMO; 2022. p. 509.
[8] Montzka SA, Myers RC, Butler JH, Elkins JW, Lock LT, Clarke AD, Goldstein AH. Observations of HFC-134a in the remote troposphere. Geophys Res Lett 1996;23(2):169–72. https://doi.org/10.1029/95GL03590.
[9] Montzka SA, McFarland M, Andersen SO, Miller BR, Fahey DW, Hall BD, Hu L, Siso C, Elkins JW. Recent trends in global emissions of hydrochlorofluorocarbons and hydrofluorocarbons: reflecting on the 2007 adjustments to the Montreal Protocol. J Phys Chem A 2015;119(19):4439–49. https://doi.org/10.1021/jp5097376.
[10] Mahieu E, Fischer EV, Franco B, Palm M, Wizenberg T, Smale D, Clarisse L, Clerbaux C, Coheur PF, Hannigan JW, Lutsch E, Notholt J, Pardo Cantos I, Prignon M, Servais C, Strong K. First retrievals of peroxyacetyl nitrate (PAN) from ground-based FTIR solar spectra recorded at remote sites, comparison with model and satellite data. Elem Sci Anth 2021;9(1):00027. https://doi.org/10.1525/elementa.2021.00027.
[11] Zander R, Mahieu E, Demoulin P, Duchatelet P, Roland G, Servais C, De Mazière M, Reimann S, Rinsland CP. Our changing atmosphere: evidence based on long-term infrared solar observations at the Jungfraujoch since 1950. Sci Total Environ 2008;391(2–3):184–95. https://doi.org/10.1016/j.scitotenv.2007.10.018.
[12] De Mazière M, Thompson AM, Kurylo MJ, Wild JD, Bernhard G, Blumenstock T, Braathen GO, Hannigan JW, Lambert JC, Leblanc T, McGee TJ, Nedoluha G, Petropavlovskikh I, Seckmeyer G, Simon PC, Steinbrecht W, Strahan SE. The Network for the Detection of Atmospheric Composition Change (NDACC): history, status and perspectives. Atmos Chem Phys 2018;18(7):4935–64. https://doi.org/10.5194/acp-18-4935-2018.
[13] Reimann S, Vollmer MK, Hill M, Schlauri P, Guillevic M, Brunner D, Henne S, Rust D, Emmenegger L. Long-term observations of atmospheric halogenated organic trace gases. Chimia 2020;74(3):136. https://doi.org/10.2533/chimia.2020.136.
[14] Prinn RG, Weiss RF, Arduini J, Arnold T, DeWitt HL, Fraser PJ, et al. History of chemically and radiatively important atmospheric gases from the Advanced Global Atmospheric Gases Experiment (AGAGE). Earth Syst Sci Data 2018;10(2):985–1018. https://doi.org/10.5194/essd-10-985-2018.
[15] Simmonds PG, O'Doherty S, Nickless G, Sturrock GA, Swaby R, Knight P, Ricketts J, Woffendin G, Smith R. Automated gas chromatograph/mass spectrometer for routine atmospheric field measurements of the CFC replacement compounds, the hydrofluorocarbons and hydrochlorofluorocarbons. Anal Chem 1995;67(4):717–23. https://doi.org/10.1021/ac00100a005.
[16] Miller BR, Weiss RF, Salameh PK, Tanhua T, Greally BR, Mühle J, Simmonds PG. Medusa: a sample preconcentration and GC/MS detector system for in situ measurements of atmospheric trace halocarbons, hydrocarbons, and sulfur compounds. Anal Chem 2008;80(5):1536–45. https://doi.org/10.1021/ac702084k.
[17] O'Doherty S, Simmonds PG, Cunnold DM, Wang HJ, Sturrock GA, Fraser PJ, Ryall D, Derwent RG, Weiss RF, Salameh P, Miller BR, Prinn RG. In situ chloroform measurements at Advanced Global Atmospheric Gases Experiment atmospheric research stations from 1994 to 1998. J Geophys Res: Atmos 2001;106(D17):20429–44. https://doi.org/10.1029/2000JD900792.
[18] Cunnold DM, Steele LP, Fraser PJ, Simmonds PG, Prinn RG, Weiss RF, et al. In situ measurements of atmospheric methane at GAGE/AGAGE sites during 1985–2000 and resulting source inferences. J Geophys Res: Atmos 2002;107(D14). https://doi.org/10.1029/2001JD001226. ACH-20.
[19] Bernath PF, McElroy CT, Abrams MC, Boone CD, Butler M, Camy-Peyret C, Carleer M, Clerbaux C, Coheur PF, Colin R, DeCola P, De Mazière M, Drummond JR, Dufour D, Evans WFJ, Fast H, Fussen D, Gilbert K, Jennings DE, Llewellyn EJ, Lowe RP, Mahieu E, McConnell JC, McHugh M, McLeod SD, Michaud R, Midwinter C, Nassar R, Nichitiu F, Nowlan C, Rinsland CP, Rochon YJ, Rowlands N, Semeniuk K, Simon P, Skelton R, Sloan JJ, Soucy MA, Strong K, Tremblay P, Turnbull D, Walker KA, Walkty I, Wardle DA, Wehrle V, Zander R, Zou J. Atmospheric chemistry experiment (ACE): mission overview. Geophys Res Lett 2005;32(15). https://doi.org/10.1029/2005GL022386.
[20] Fernando AM, Bernath PF, Boone CD. Trends in atmospheric HFC-23 (CHF_3) and HFC-134a abundances. J Quant Spectros Radiat Transf 2019;238:106540. https://doi.org/10.1016/j.jqsrt.2019.06.019.
[21] Boone CD, Bernath PF, Lecours M. Version 5 Retrievals for ACE-FTS and ACE-Imagers. J Quant Spectrosc Radiat Transf 2023:108749. https://doi.org/10.1016/j.jqsrt.2023.108749.
[22] Chipperfield MP. New version of the TOMCAT/SLIMCAT off-line chemical transport model: intercomparison of stratospheric tracer experiments. Q J R Meteorol Soc: J Atmos Sci Appl Meteorol Phys Oceanogr 2006;132(617):1179–203. https://doi.org/10.1256/qj.05.51.
[23] Hersbach H, Bell B, Berrisford P, Hirahara S, Horányi A, Muñoz-Sabater J, et al. The ERA5 global reanalysis. Q J R Meteorol Soc 2020;146(730):1999–2049. https://doi.org/10.1002/qj.3803.
[24] World Meteorological Organization (WMO). GAW Report No. 58. Geneva: WMO; 2018. p. 588.
[25] Clerbaux C, Colin R, Simon PC, Granier C. Infrared cross sections and global warming potentials of 10 alternative hydrohalocarbons. J Geophys Res: Atmos 1993;98(D6):10491–7. https://doi.org/10.1029/93JD00390.
[26] Highwood EJ, Shine KP. Radiative forcing and global warming potentials of 11 halogenated compounds. J Quant Spectros Radiat Transf 2000;66(2):169–83. https://doi.org/10.1016/S0022-4073(99)00215-0.
[27] Nemtchinov V, Varanasi P. Absorption cross-sections of HFC-134a in the spectral region between 7 and 12μm. J Quant Spectros Radiat Transf 2004;83(3-4):285–94. https://doi.org/10.1016/S0022-4073(02)00356-4.
[28] Sharpe SW, Johnson TJ, Sams RL, Chu PM, Rhoderick GC, Johnson PA. Gas-phase databases for quantitative infrared spectroscopy. Appl Spectrosc 2004;58(12):1452–61. https://doi.org/10.1366/0003702042641281.
[29] Gohar LK, Myhre G, Shine KP. Updated radiative forcing estimates of four halocarbons. J Geophys Res: Atmos 2004;109(D1). https://doi.org/10.1029/2003JD004320.
[30] Harrison JJ. Infrared absorption cross sections for 1, 1, 1, 2-tetrafluoroethane. J Quant Spectrosc Radiat Transf 2015;151:210–6. https://doi.org/10.1016/j.jqsrt.2014.09.023.
[31] Rodgers CD. Inverse methods for atmospheric sounding: theory and practice. World Scientific 2000;2.
[32] Gordon IE, Rothman LS, Hargreaves RJ, Hashemi R, Karlovets EV, Skinner FM, et al. The HITRAN2020 molecular spectroscopic database. J Quant Spectrosc Radiative Transf 2022;277:107949. https://doi.org/10.1016/j.jqsrt.2021.107949.
[33] Gettelman A, Mills MJ, Kinnison DE, Garcia RR, Smith AK, Marsh DR, et al. The Whole Atmosphere Community Climate Model Version 6 (WACCM6). J Geophys Res: Atmos 2019;124(23):12380–403. https://doi.org/10.1029/2019JD030943.
[34] Berrisford P, Dee D, Poli P, Brugge R, Fielding K, Fuentes M, et al. The ERA-Interim archive Version 2.0, Shinfield Park. Reading 2011;1:23.
[35] Prignon M, Chabrillat S, Minganti D, O'Doherty S, Servais C, Stiller G, Toon GC, Vollmer MK, Mahieu E. Improved FTIR retrieval strategy for HCFC-22 ($CHClF_2$), comparisons with in situ and satellite datasets with the support of models, and determination of its long-term trend above Jungfraujoch. Atmos Chem Phys 2019;19(19):12309–24. https://doi.org/10.5194/acp-19-12309-2019.
[36] Barthlott S, Schneider M, Hase F, Wiegele A, Christner E, González Y, Blumenstock T, Dohe S, García O, Sepúlveda E, Strong K, Mendonca J, Weaver D, Palm M, Deutscher NM, Warneke T, Notholt J, Lejeune B, Mahieu E, Jones N, Griffith DWT, Velazco VA, Smale D, Robinson J, Kivi R, Heikkinen P, Raffalski U. Using XCO_2 retrievals for assessing the long-term consistency of NDACC/FTIR data sets. Atmos Meas Tech 2015;8:1555–73. https://doi.org/10.5194/amt-8-1555-2015.
[37] Pardo Cantos I, Mahieu E, Chipperfield MP, Smale D, Hannigan JW, Friedrich M, et al. Determination and analysis of time series of CFC-11 (CCl_3F) from FTIR solar spectra, in situ observations, and model data in the past 20 years above Jungfraujoch (46°N), Lauder (45°S), and Cape Grim (40°S) stations. Environ Sci Atmos 2022;2(6):1487–501. https://doi.org/10.1039/D2EA00060A.
[38] Sussmann R, Borsdorff T, Rettinger M, Camy-Peyret C, Demoulin P, Duchatelet P, Mahieu E, Servais C. Harmonized retrieval of column-integrated atmospheric water vapor from the FTIR network – first examples for long-term records and station trends. Atmos Chem Phys 2009;9(22):8987–99. https://doi.org/10.5194/acp-9-8987-2009.
[39] Friedrich M, Smeekes S, Urbain JP. Autoregressive wild bootstrap inference for nonparametric trends. J Econom 2020;214(1):81–109. https://doi.org/10.1016/j.jeconom.2019.05.006.
[40] Bernath PF, Crouse J, Hughes RC, Boone CD. The Atmospheric Chemistry Experiment Fourier Transform Spectrometer (ACE-FTS) version 4.1 retrievals: trends and seasonal distributions. J Quant Spectros Radiat Transf 2021;259:107409. https://doi.org/10.1016/j.jqsrt.2020.107409.
[41] Zander R, Duchatelet P, Mahieu E, Demoulin P, Roland G, Servais C, Auwera JV, Perrin A, Rinsland CP, Crutzen PJ. Formic acid above the Jungfraujoch during 1985–2007: observed variability, seasonality, but no long-term background evolution. Atmos Chem Phys 2010;10(20):10047–65. https://doi.org/10.5194/acp-10-10047-2010.
[42] Gardiner T, Forbes A, De Mazière M, Vigouroux C, Mahieu E, Demoulin P, Velazco V, Notholt J, Blumenstock T, Hase F, Kramer I, Sussmann R, Stremme W, Mellqvist J, Strandberg A, Ellingsen K, Gauss M. Trend analysis of greenhouse gases over Europe measured by a network of ground-based remote FTIR instruments. Atmos Chem Phys 2008;8(22):6719–27. https://doi.org/10.5194/acp-8-6719-2008.